

Article

Development of Innovative Structured Catalysts for the Catalytic Decomposition of N₂O at Low Temperatures

Eugenio Meloni ^{1,*}, Marco Martino ¹, Simona Renda ¹, Olga Muccioli ¹, Pluton Pullumbi ², Federico Brandani ² and Vincenzo Palma ¹

¹ Department of Industrial Engineering, University of Salerno, Via Giovanni Paolo II 132, 84084 Fisciano, Italy

² Air Liquide, Paris Innovation Campus. 1, Chemin de la Porte des Loges, 78350 Les Loges en Josas, France

* Correspondence: emeloni@unisa.it

Abstract: Nitrous oxide (N₂O), produced from several human activities, is considered a greenhouse gas with significant environmental impacts. The most promising abatement technology consists of the catalytic decomposition of N₂O into nitrogen and oxygen. Many recently published papers dealing with N₂O catalytic decomposition over Ni-substituted Co₃O₄ are related to the treatment of N₂O concentrations less than 2 vol% in the feed stream. The present work is focused on developing catalysts active in the presence of a gaseous stream richer in N₂O, up to 20 vol%, both as powder and in structured configurations suitable for industrial application. With this aim, different nickel-cobalt mixed oxides (Ni_xCo_{1-x}Co₂O₄) were prepared, characterized, and tested. Subsequently, since alumina-based slurries assure successful deposition of the catalytic species on the structured carrier, a screening was performed on three nickel-cobalt-alumina mixed oxides. As the latter samples turned out to be excellent catalysts for the N₂O decomposition reaction, the final catalytic formulation was transferred to a silicon carbide monolith. The structured catalyst led to the following very promising results: total N₂O conversion and selectivity towards N₂ and O₂ were reached at 510 °C by feeding 20 vol% of N₂O. It represents an important achievement in the view of developing a more concretely applicable catalytic system for industrial processes.

Keywords: structured catalysts; catalytic decomposition of N₂O; high selective catalysts; process intensification



Citation: Meloni, E.; Martino, M.; Renda, S.; Muccioli, O.; Pullumbi, P.; Brandani, F.; Palma, V. Development of Innovative Structured Catalysts for the Catalytic Decomposition of N₂O at Low Temperatures. *Catalysts* **2022**, *12*, 1405. <https://doi.org/10.3390/catal12111405>

Academic Editors: Hugo de Lasa and Mohammad Mozahar Hossain

Received: 7 September 2022

Accepted: 8 November 2022

Published: 10 November 2022

Publisher's Note: MDPI stays neutral with regard to jurisdictional claims in published maps and institutional affiliations.



Copyright: © 2022 by the authors. Licensee MDPI, Basel, Switzerland. This article is an open access article distributed under the terms and conditions of the Creative Commons Attribution (CC BY) license (<https://creativecommons.org/licenses/by/4.0/>).

1. Introduction

Environmental issues such as pollution [1], global warming, and ozone layer depletion are of universal concern. One compound previously not associated with these issues is nitrous oxide (N₂O). In the past years, it has not been recognized as a harmful species nor has received the appropriate consideration from the scientific community due to the undervaluation of its detrimental effect on the environment [2]. The N₂O contribution equals 6% of the total greenhouse gas emissions, and its global warming potential (GWP) of 310 corresponds to 21 times that of CO₂ and CH₄, respectively.

During the last decade, owing to the constant increase in its concentration in the atmosphere, both from natural and anthropogenic sources (0.2–0.3% per year) and its long atmospheric residence time (110–150 years) [3], a growing interest was paid to this topic. In any case, effective mitigation for N₂O emissions requires an understanding of its sources.

Substantial quantities of N₂O are produced from anthropogenic activities (Figure 1), such as the production of chemicals (adipic acid, nitric acid, acrylonitrile, nylon, and caprolactame), road vehicles, medical exhausts [4], the incomplete combustion of fossil fuels and biomass, and the nitrification and denitrification processes [5,6].

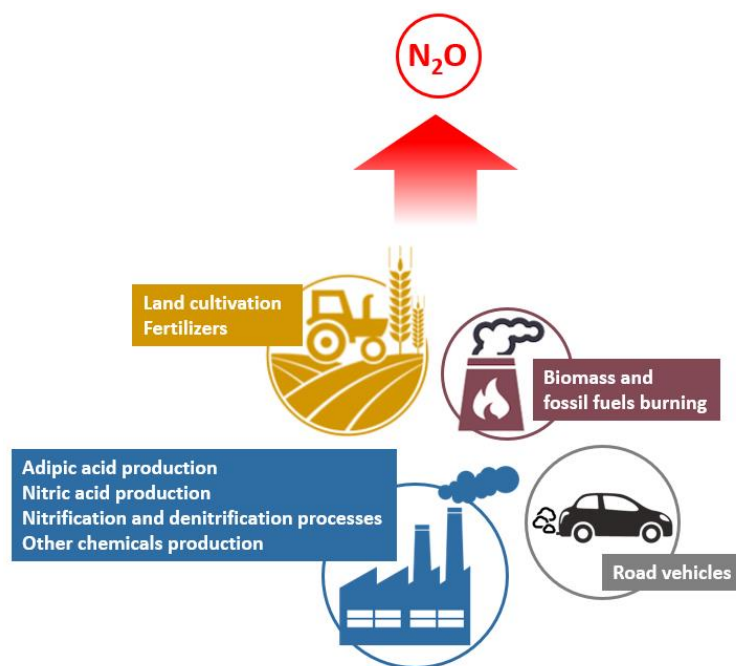


Figure 1. Main anthropogenic sources of N_2O .

The different contributions of the anthropogenic sources of N_2O are reported in Figure 2.

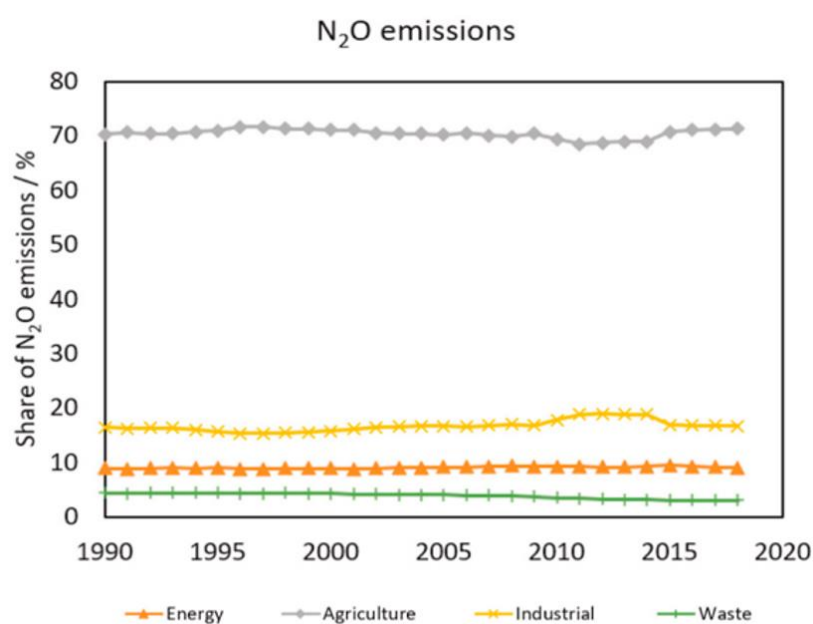


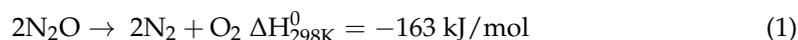
Figure 2. Share of N_2O emissions by sector, from 1990 to 2018 [7].

Since the N_2O emissions continue to increase and the atmospheric levels are expected to double by 2050 [8], the abatement of N_2O has aroused interest from both the scientific community and industry. N_2O removal can be obtained by means of different methods, such as adsorption processes and thermal and catalytic decomposition.

The high efficiency and low cost of the catalytic N_2O decomposition to nitrogen and oxygen make this technique one of the most attractive, as well as its process simplicity [8].

Generally, the catalytic decomposition of N_2O occurs via electron donation from the catalyst to the antibonding orbital of N_2O , leading to N-O bond scission and N_2 and O_2 formation [8,9]. The catalytic decomposition of N_2O is a direct exothermic reaction

(Equation (1)) kinetically limited, so the selection of a suitable catalyst is essential to promote the N-O bond breakup [10,11].



Over time, many scientific papers have been published about catalytic decomposition, and several catalysts have been studied [12]. The industrial applications of zeolite-based systems [13] have been drastically reduced due to the unfavorable behavior of these materials in the presence of different substances contained in the gas stream, in particular the poisoning by SO_2 [14]. Among the noble metals, rhodium (Rh) and ruthenium (Ru) are the most active for the decomposition of N_2O at low temperatures, but their performance is strongly affected by the oxygen concentration in the feed stream [15]. Moreover, the high cost limits their application in the industry [16]. On the other hand, transition metal oxides such as CuO , NiO , Co_3O_4 , and Fe_3O_4 , which are characterized by low price and good catalytic activity, have received extensive attention for application in N_2O catalytic decomposition [11,17]. Among them, the Co_3O_4 -based catalysts have shown better catalytic performance, also at low-temperature conditions, and are promising candidates for the N_2O decomposition reaction, due to their relatively high redox capacity and the weakness of the metal-oxygen bond [8,18,19]. Particularly, the cobalt spinel $\text{Co}^{\text{II}}\text{Co}^{\text{III}}_2\text{O}_4$ and its derivatives obtained by partial substitution with 2p, 3d, and 4f dopants have created great interest [20,21]. It is demonstrated that a synergistic effect between Co and transition metals can be obtained by a partial replacement of Co^{2+} with Ni^{2+} , Cu^{2+} , Zn^{2+} , or other transition metals in the tricobalt tetraoxide (Co_3O_4), enhancing the N_2O decomposition reaction [3,22,23]. These materials' class results are beneficial for the decomposition reaction, due to the involvement of different metal atoms and oxidation states whose combination leads to suitable properties [21,23].

Xue et al. [24] explored the influence of CeO_2 on the catalytic activity of Co_3O_4 . The presence of CeO_2 promoted the desorption of oxygen atoms from the active sites favoring the reduction of Co^{3+} to Co^{2+} and enhancing the N_2O decomposition reaction. Wang et al. [25] demonstrated that the enhancement of the electron donation ability of Co^{2+} is due to the interaction between Sn and Co oxides at the $\text{SnO}_2/\text{Co}_3\text{O}_4$ interface.

Interesting works are those of Yan et al. [3,23], who tested several spinel catalysts, namely, $\text{Mg}_x\text{Co}_{1-x}\text{Co}_2\text{O}_4$, $\text{Ni}_x\text{Co}_{1-x}\text{Co}_2\text{O}_4$, and $\text{Zn}_x\text{Co}_{1-x}\text{Co}_2\text{O}_4$ with $x = 0.0\text{--}0.99$, for the decomposition of N_2O . They demonstrated how the catalytic performance was dependent on the degree of Co^{2+} substitution by the other metals. The results showed that $\text{Mg}_{0.54}\text{Co}_{0.46}\text{Co}_2\text{O}_4$, $\text{Ni}_{0.74}\text{Co}_{0.26}\text{Co}_2\text{O}_4$, and $\text{Zn}_{0.36}\text{Co}_{0.64}\text{Co}_2\text{O}_4$ exhibited the highest activities. Abu-Zied et al. [26] study indicated that mixed $\text{NiO-Co}_3\text{O}_4$ catalysts had better catalytic properties with respect to separated NiO and Co_3O_4 , highlighting the synergistic effect between the compounds.

The papers dealing with N_2O catalytic decomposition over Ni-substituted Co_3O_4 available in the present literature are related to the treatment of low N_2O concentrations, i.e., less than 2 vol% in the reagent mixture. An interesting breakthrough could be achieved with the development of a catalytic formulation able to successfully treat feeding streams containing high concentrations of N_2O , such as in the case of adipic acid production plants [27]. This catalytic system could be applied either directly in the treatment of the tail gases exiting from the plant or after a regeneration stage of an N_2O adsorption process that returns a gas stream rich in N_2O . To this end, in the present work, different nickel-cobalt mixed oxides ($\text{Ni}_x\text{Co}_{1-x}\text{Co}_2\text{O}_4$), active for the N_2O decomposition reaction, were prepared, characterized, and tested employing reagent mixtures containing concentrations of N_2O from 5 up to 20 vol%. In addition, it could be interesting to perform more practical catalytic configurations, such as monolithic systems, suitable for industrial applications. Indeed, the use of monoliths allows having many advantages, among which is the possibility to treat high gas volumes with low-pressure drop operations, as well as the elimination of mass transport limitations [28–30]. Therefore, aiming at the development of a structured catalyst, which requires an alumina-based washcoat to effectively deposit the active species [31],

additional catalytic powder samples were investigated, by modifying the formulation with Al_2O_3 . The nickel-cobalt-alumina mixed oxides samples turned out to be excellent catalysts for the N_2O decomposition reaction; indeed, total conversion of N_2O and a selectivity of 100% toward N_2 and O_2 were reached at a temperature lower than $450\text{ }^\circ\text{C}$ to treat a feeding mixture containing 20 vol% of N_2O . Furthermore, as widely reported [1,3,22], the oxygen inhibits the decomposition reaction and its adsorption leads to the poisoning of the catalyst; therefore, the effect of the presence of oxygen in the reagent mixture on the catalytic performance was investigated, also because oxygen is often present in tail gases from adipic acid production plants, for example. In conclusion, the most promising Al_2O_3 -modified catalytic formulation was deposited on a silicon carbide (SiC) honeycomb monolith to carry out a structured catalyst. The results demonstrated that the transition from the powder to the structured configuration, by choosing the operating conditions in order to assure the same contact time in both systems, did not lead to a great worsening of the catalytic performance, or rather, with the monolithic structured catalyst, total conversion of N_2O and selectivity of 100% toward N_2 and O_2 were achieved at $510\text{ }^\circ\text{C}$.

2. Results and Discussion

2.1. Catalysts Characterization

The BET-specific surface area (SSA), pore volume, and average pore radius of the samples as obtained through N_2 adsorption at $-196\text{ }^\circ\text{C}$ are given in Table 1. The results retrieved for samples NiCo_1 and NiCo_2 highlight how the employment of different precipitating agents can lead to different textural properties. Particularly, comparing the samples NiCo_1 and NiCo_2, it is evident that the use of Na_2CO_3 is detrimental with respect to the porous structure of the sample. The alumina-containing catalysts showed different SSA values, depending on both the Al_2O_3 contents and the preparation method. In detail, for what concerns the samples prepared using an alumina-based washcoat, the higher the alumina loading was, the higher the SSA value was, while the average pore dimension was similar for the three samples. On the other hand, the catalyst NiCoAl_C prepared by coprecipitation of Co, Ni, and Al precursors achieved an SSA value lower than the other alumina-based samples. Since NiCoW10%, NiCoW15%, and NiCoW30% are derived from a mixture of NiCo_1 and alumina, their SSA is strictly linked to the one of the pseudoboehmite used to prepare the slurry. On the contrary, in the case of the NiCoAl_C sample, the SSA value does not depend on the alumina content, but it is associated with the chemical structure reached through the preparation method. Moreover, NiCoAl_C highlighted the highest average pore radius.

Table 1. SSA, pore volume, pore radius, Ni/Co ratio, and Al_2O_3 content about the catalytic powder samples.

| Sample | SSA (m^2/g) | Pore Volume (cm^3/g) | Pore Radius (nm) | Ni/Co | Al_2O_3 (wt%) |
|-----------|----------------------------------|---|---------------------|-------|----------------------------------|
| NiCo_1 | 53 | 0.130 | 5.95 | 0.32 | - |
| NiCo_2 | 29 | 0.040 | 1.70 | 0.33 | - |
| NiCo_W10% | 57 | 0.187 | 2.60 | 0.32 | 9.6 |
| NiCo_W15% | 59 | 0.169 | 2.79 | 0.32 | 14.6 |
| NiCo_W30% | 64 | 0.115 | 3.55 | 0.32 | 28.4 |
| NiCoAl_C | 40 | 0.180 | 6.00 | 0.40 | 14.5 |

The analytical technique XRF was applied with the aim of determining the effective Ni/Co ratio and the alumina content inside the alumina-based powder catalysts. As a result, all the values are in fair agreement with the expected ones, except for NiCoAl_C. The three alumina-based samples showed the same Ni/Co ratio as NiCo_2 used for the preparation, while NiCoAl_C originates from a coprecipitation of the precursor salts NiCoAl_C sample showed a higher Ni/Co ratio due to the different preparation method.

The SEM results about the powder samples are shown in Figure 3.

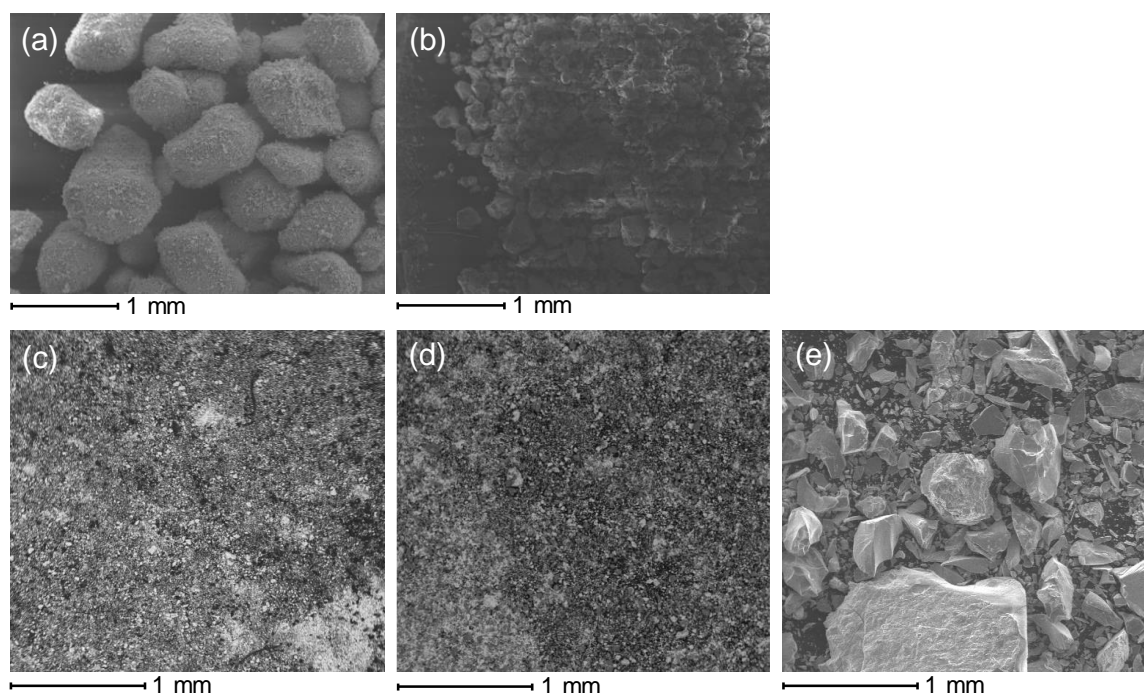


Figure 3. SEM images: (a) NiCo_1, (b) NiCo_2, (c) NiCo_W10%, (d) NiCo_W30%, and (e) NiCoAl_C.

The catalysts have the following different structures: (a) NiCo_1 exhibits a granular structure, while (b) NiCo_2 shows a dusty structure. The samples prepared with the 10% (c) and 30% (d) of alumina have a similar structure, different from the coprecipitate catalyst (e), which shows a more compact structure.

All the samples have an excellent distribution of the species, and, from the EDX images relative to the sample NiCo_2 (Figure 4), it is possible to observe the presence of sodium (Na) to indicate that during the preparation phase, the washing of the resultant precipitate did not eliminate the Na_2CO_3 species used as a precipitating agent.

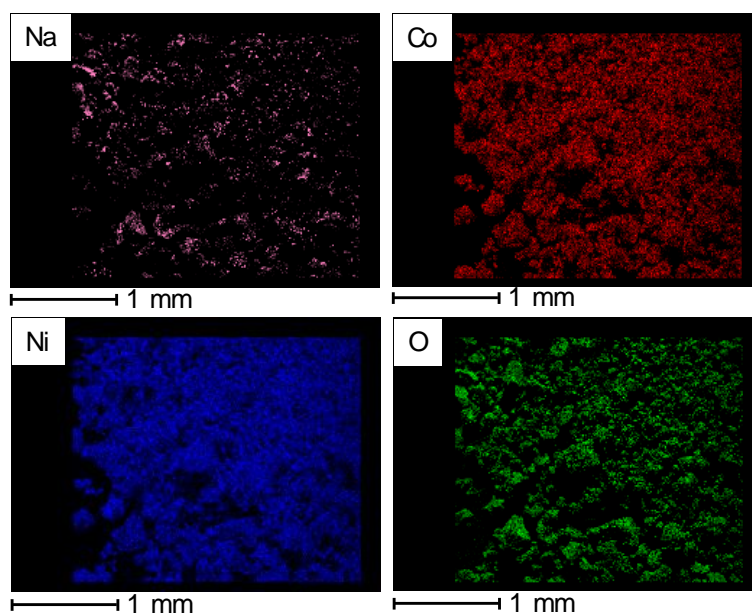


Figure 4. EDX mapping relative to sample NiCo_2.

In Figure 5, the SEM/EDX result about the structured sample, namely, NiCoAl_C_SiC, is shown. The images highlight a homogeneous distribution of the slurry on the monolithic surface.

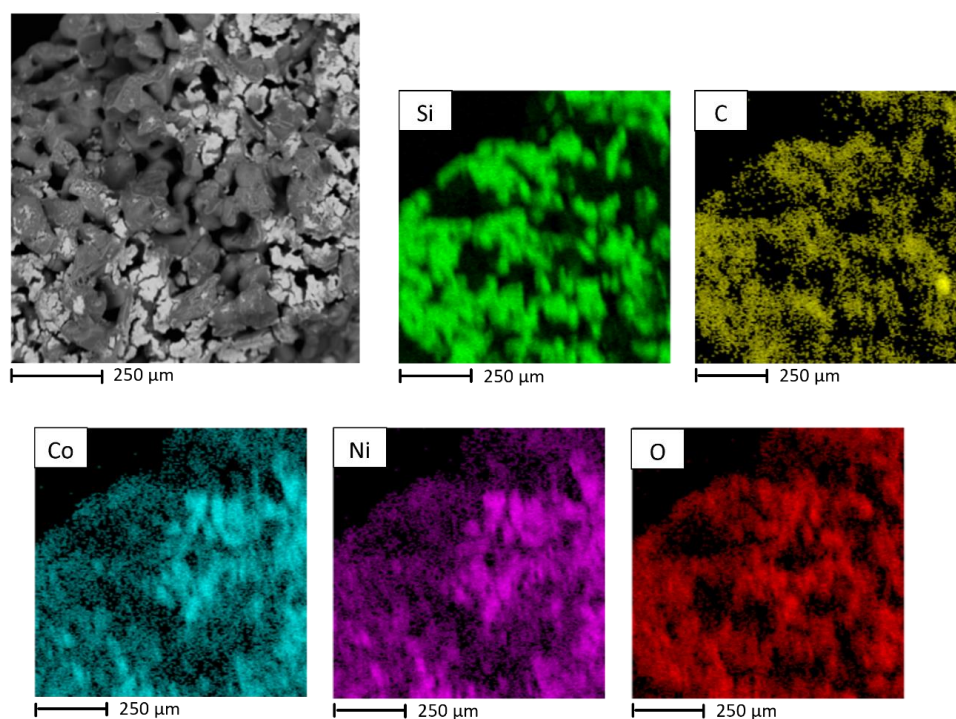


Figure 5. SEM/EDX images relative to sample NiCoAl_C_SiC.

In Figure 6, the XRD diffractograms show that NiCo_1 and NiCo_2 samples are characterized by a spinel structure where Ni^{2+} substitutes Co^{2+} to form $\text{Ni}_x\text{Co}_{1-x}\text{Co}_2\text{O}_4$ oxide, according to literature data [3]. The NiCoAl_C sample exhibits an XRD pattern typical of a trimetallic spinel structure [32], where the peaks seem to be slightly shifted to higher angles compared to the previous samples. This shift could be attributed to the change in lattice parameters due to the incorporation of Al into the oxide structure [33].

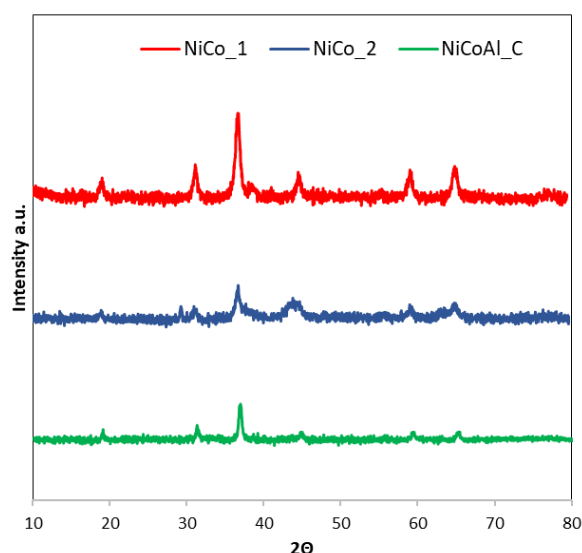


Figure 6. XRD patterns of NiCo_1, NiCo_2, NiCoAl_C samples.

The Raman spectra of the samples (Figure 7) confirm the composition and the structure already shown by XRD results [34–36]. In particular, NiCoAl_C and the NiCo-based catalysts exhibit Raman spectra with similar features highlighting the characteristic peaks of NiCo trimetallic and bimetallic spinel oxide structures, respectively [37].

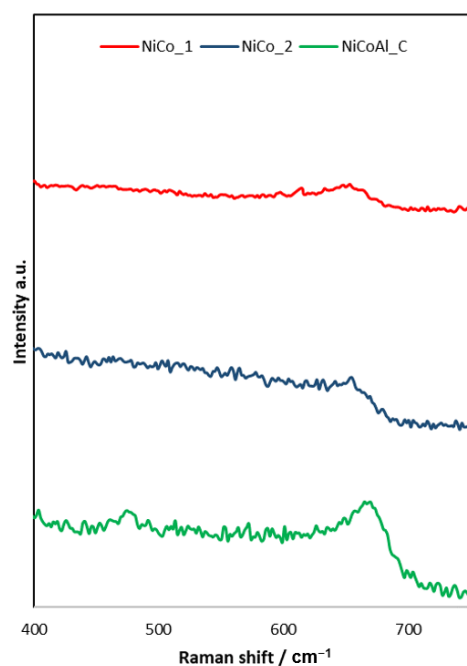


Figure 7. Raman spectrum of NiCo_1, NiCo_2, NiCoAl_C samples.

TPD experimental tests have been performed over NiCoAl_C and NiCo_1 by using N₂O (Figure 8). The results have shown that the following two peaks relevant to O₂ desorption are visible for both samples: the first peak occurs at a temperature between 100 °C and 400 °C and is ascribable to the desorption of weaker chemisorbed oxygen; the second peak obtained over 400 °C is attributable to the oxygen desorption due to the thermal effect [22]. Furthermore, the aluminum-modified catalyst exhibits a lower amount of desorbed oxygen compared to the sample without alumina, giving an indication about the catalytic behavior of the samples. After the interaction between the N₂O and the catalysts, a certain amount of oxygen remains adsorbed on the surface. The lower oxygen desorption obtained with the NiCoAl_C is related to a smaller number of active sites occupied by oxygen, explaining the major catalytic activity of the catalyst. This result is in line with the reaction mechanisms as follows: the N₂O molecule adsorbs on the surface of the catalyst, leading to the breakage of the N–O bond, giving gaseous N₂, then two adsorbed oxygen atoms react with each other according to the Langmuir–Hinshelwood mechanism or one adsorbed oxygen atom reacts with the gaseous N₂O molecule to produce O₂, following the Eley–Rideal mechanism [9].

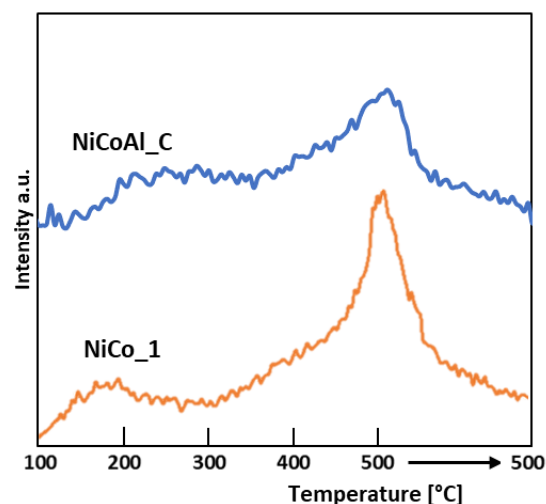


Figure 8. N₂O-TPD over NiCo_1 and NiCoAl_C catalysts.

Figure 9 shows the results obtained from the ultrasound adherence test performed on the structured catalyst. The percentage weight loss has been calculated weighted the sample after each cycle of bath, according to Equation (2).

$$\text{Weight loss} = \frac{\text{Initial mass} - \text{final mass}}{\text{Initial washcoat mass}} \quad (2)$$

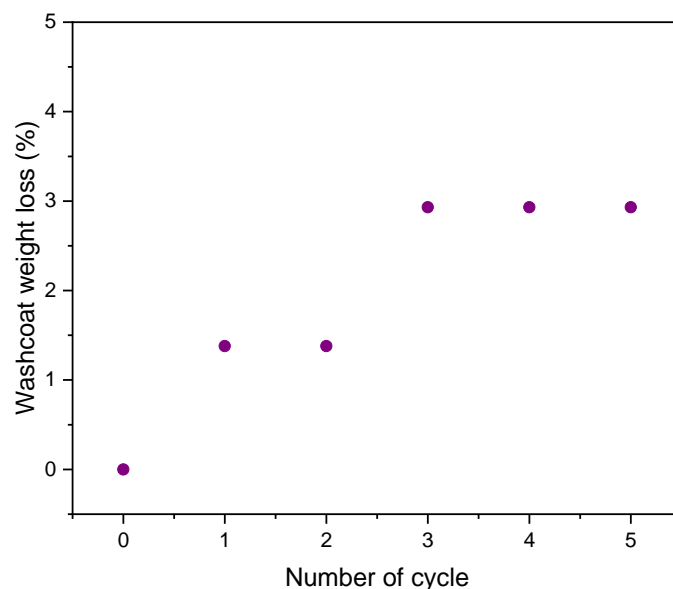


Figure 9. Ultrasound adhesion test performed on NiCoAl_C_SiC structured sample.

The total number of cycles was established considering the results obtained during the tests as follows: in fact, when the weight variation between two consecutive cycles is null, the test can be considered concluded. The NiCoAl_C_SiC sample subjected to the ultrasound stress demonstrated that the chemical support adhered with excellent stability to the SiC carrier; indeed, after 5 cycles, the total weight loss is about 3%, a value lower than that observed in literature for similarly structured catalysts.

2.2. Ni-Co_Based Catalysts Activity Test

2.2.1. Powder Catalysts

At first, the N₂O catalytic decomposition was evaluated over the NiCo samples in order to identify the most attractive precipitating agent. This preliminary screening was performed using a GHSV of 15,000 h⁻¹, in the presence of oxygen, and in the presence of two different feed streams, respectively containing 10 vol% and 5 vol% of N₂O. The outcomes, in terms of N₂O conversion, are reported in Figure 10. From the trend in conversion, it is clear that the precipitating agent used during the preparation procedure had a strong influence on the catalytic performances of the samples. This can be adequately ascribed to the change in the textural properties of the samples. In particular, the sample NiCo_1, which exhibited the best N₂O conversion over the whole temperature range, was the one having the highest both SSA value and pore volume. The evaluation of the activity of the best sample, namely, NiCo_1, was also performed considering the effect of N₂O content. In particular, a feeding mixture containing 5 vol% N₂O and 5 vol% O₂ in Ar, keeping unchanged the other operating conditions, was fed. The outcomes, reported in Figure 10b, showed that the change in N₂O concentration led to a worsening in the catalytic performances. This suggests that NiCo_1 can be suitable for the treatment of high N₂O concentration streams. Therefore, the ammonia solution was selected as a precipitating agent, and therefore NiCo_1 was selected as the best option to efficiently conduct the catalytic N₂O decomposition, and further modifications and experimental evaluations were performed employing this sample as a starting point.

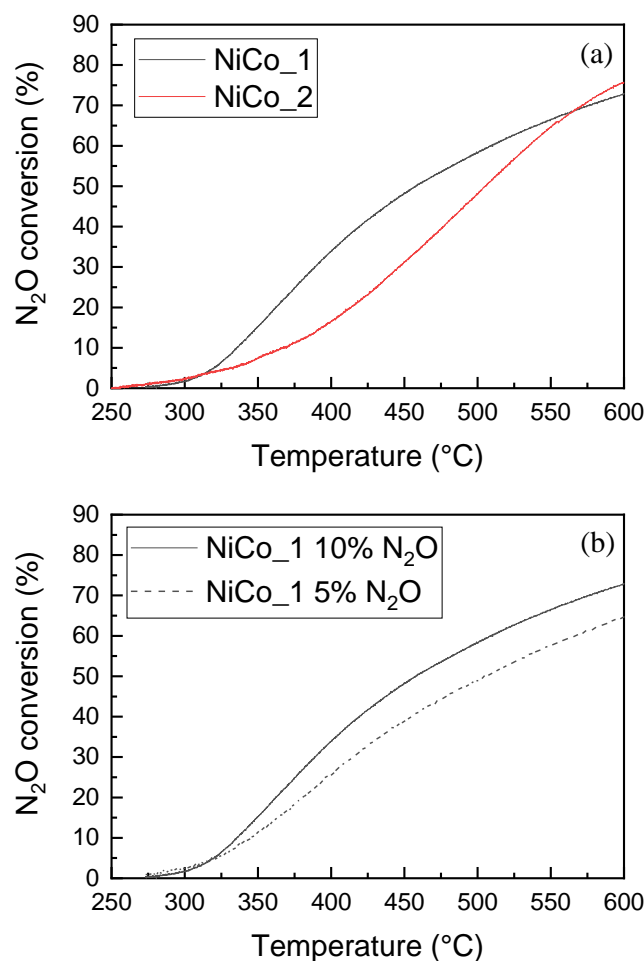


Figure 10. Catalytic performances of NiCo samples. Operating conditions: GHSV = 15,000 h⁻¹, 1 atm, (a) N₂O and O₂ 10 vol% in Ar; (b) N₂O and O₂ 5 vol% and 10 vol% in Ar, GHSV = 15,000 h⁻¹.

Effect of Alumina on the Catalytic Activity

To the aim of selecting a formulation that could be suitable for the preparation of structured catalysts, different loadings of alumina were added to the NiCo_1 sample, following two different preparation approaches, the washcoat slurry preparation, and the coprecipitation. The effect of alumina on the catalytic activity performance was first investigated in the previously adopted operating conditions, comparing the NiCo_1 catalyst with the sample modified with washcoat (having an overall alumina loading of 10 wt%) by feeding a stream with 10 vol% of N₂O. The results, shown in Figure 11a, highlighted that the presence of alumina did not determine particular modifications at low temperatures but had a marked influence above 450 °C. Therefore, the addition of alumina is feasible and can also enhance the catalytic performances at high temperatures; indeed, it is well known that alumina leads to more stable catalysts with better dispersion of the active phase [29]. For this reason, different studies about N₂O decomposition over alumina-supported catalysts have been reported in the literature [38,39]. Since the molecular oxygen limits the N₂O decomposition causing the poisoning of the catalyst, catalytic activity tests in the presence and absence of O₂ on the NiCo_W10% sample were carried out, and the results are reported in Figure 11b. As shown, the presence of oxygen inhibits the decomposition reaction, according to scientific literature data. The maximum conversions at 600 °C are 89% and 92%, respectively, in the presence and absence of oxygen. It can be expected that the inhibitory effect of oxygen is strongly correlated with the competitive adsorption of molecular oxygen on active sites, hindering the decomposition of N₂O [3].

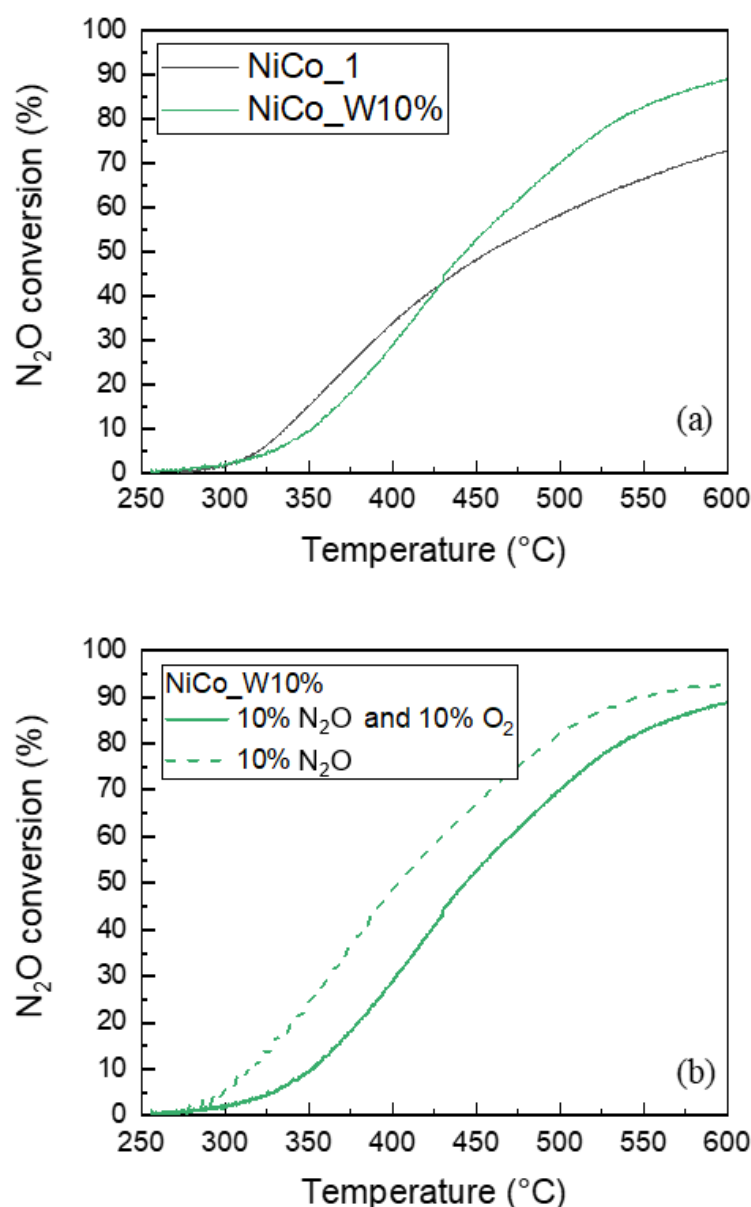


Figure 11. (a) Effect of alumina (10 wt%) addition (reagent mixture: 10 vol% N₂O, 10 vol% O₂ in Ar) and (b) effect of O₂ presence in the feed gas. Operating conditions: GHSV = 15,000 h⁻¹, 1 atm.

Figure 12 displays the comparison of the catalytic performances for the four alumina-based catalysts. The catalyst containing 10 wt% and 15 wt% of alumina showed the lowest N₂O conversion values. The other two catalysts approached a total N₂O conversion at 600 °C. Furthermore, it is possible to highlight that the increase in alumina loading enhanced the catalytic performances at high temperatures while there was a worsening in activity at low temperatures, which is coherent with the differences observed between NiCo_W10% and NiCo_1 samples. The change in the preparation method adopted, namely, the coprecipitation of the precursor salts, in the case of the NiCoAl_C sample allowed to obtain enhanced conversions both at high and low temperatures, compared to the washcoat-containing sample NiCo_WC15%, characterized by the same content of alumina. The enhancement in activity might be addressed by the incorporation of the alumina in the lattice, which leads to a distortion of the cells [33]. The different chemical structure influences the catalytic activity.

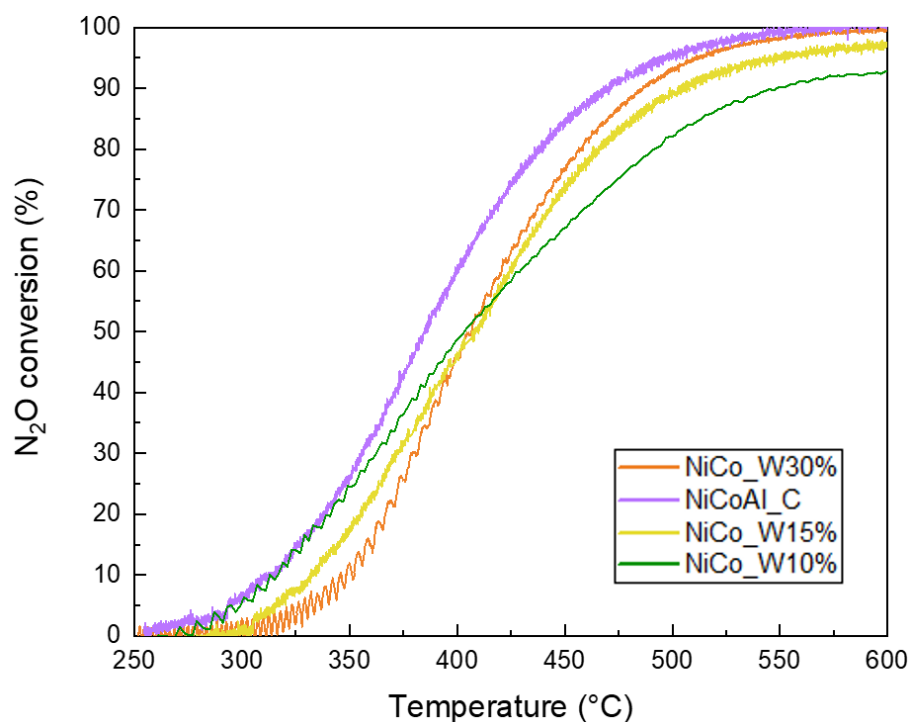


Figure 12. Activity comparison for the alumina-containing formulations. Operating conditions: GHSV = 15,000 h⁻¹, 1 atm, reagent mixture: 10 vol% N₂O in Ar.

Furthermore, the catalytic activity test performed on all the samples exhibited the total selectivity of the system toward N₂ and O₂. The results confirm that the N₂O is totally converted without any subproducts, such as NO and NO₂.

Effect of Space Velocity and N₂O Concentration

The most performant catalyst (NiCoAl_C) was tested under different GHSV conditions (15,000 h⁻¹ and 3000 h⁻¹) and at different N₂O concentrations, in order to investigate the effect of these parameters on the catalytic performances.

Figure 13a shows the results obtained in terms of N₂O conversion as follows: as expected, the lower the GHSV was, the higher the reached conversion was, whatever the operating temperature. Employing a GHSV equal to 3000 h⁻¹, the temperature necessary to reach a total N₂O conversion was lowered to 420 °C, approximately 180 °C below the temperature that was necessary using the higher GHSV value. The experimental tests have been repeated three times, and the mean deviation has been added to the figure. This was an important achievement; indeed, carrying out the N₂O decomposition reaction at a low temperature means enormous energy savings and easy management of heat within the system.

Interesting results were obtained from catalytic activity tests carried out at different N₂O compositions, as follows: 10 vol% of N₂O in Ar and 20 vol% of N₂O in Ar. The tests were performed at both low and high GHSV and are reported in Figure 13b,c for 3000 h⁻¹ and 15,000 h⁻¹, respectively. It is possible to note that if the treated stream contains up to 20 vol% of N₂O, the increase in N₂O content did not negatively influence the catalytic activity since the same conversion results were obtained. This important result indicates that it is possible to perform the catalytic N₂O decomposition at moderately low temperatures (about 420 °C) when treating highly N₂O-concentrated gaseous streams with contents up to 20 vol%.

It is important to highlight that in all the catalytic activity tests, the selectivity of the catalysts was total for N₂ and O₂, with no by-product formation.

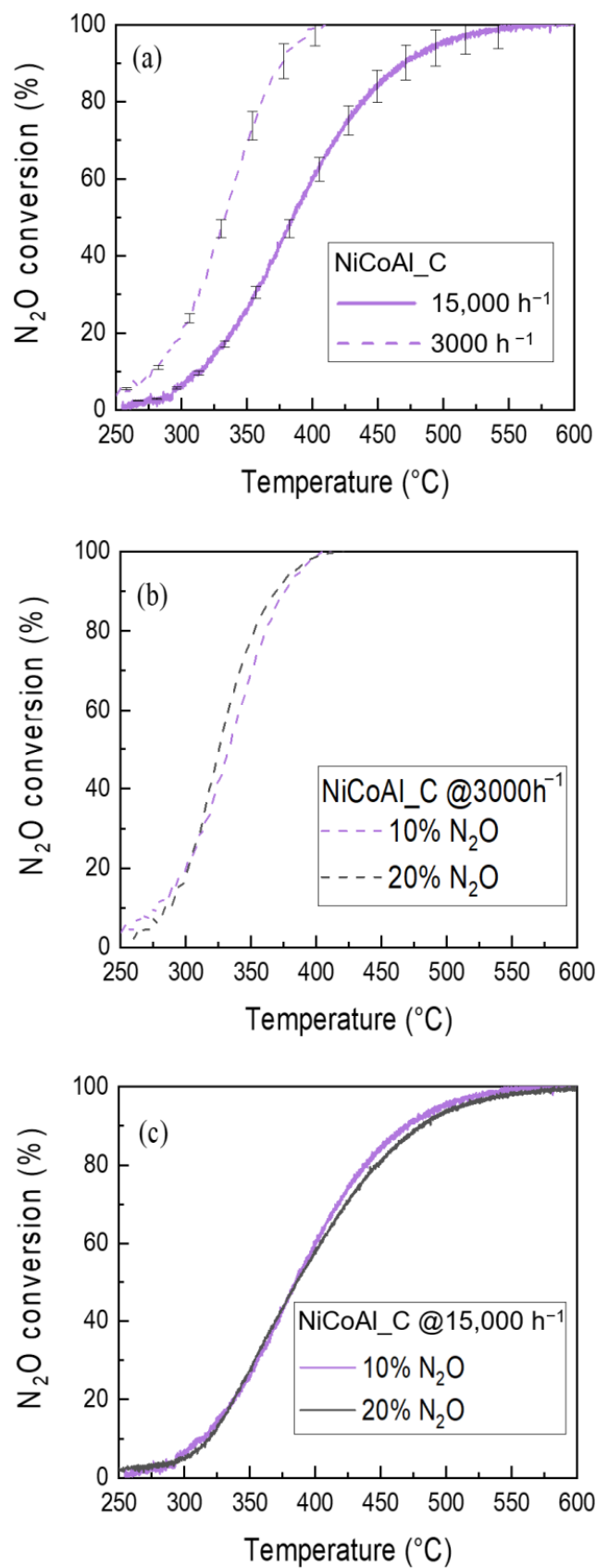


Figure 13. (a) GHSV effect in catalytic N₂O decomposition over NiCoAl_C catalyst (reagent mixture: 20 vol% N₂O in Ar); (b) effect of N₂O concentration at GHSV = 3000 h⁻¹, 1 atm; (c) effect of N₂O concentration at GHSV = 15,000 h⁻¹, 1 atm.

2.2.2. Structured Catalyst

In the following paragraph, it will be shown the effect of the SiC monolith on the catalytic performance. In Figure 14, a comparison between the powder and structured samples is illustrated. Although the NiCoAl_C_SiC sample exhibits a slight worsening of the catalytic performance at the same operating condition used for the powder, it is possible to note that the employment of a structured carrier, thus a more practical configuration, allows reaching an N₂O conversion of 99% at 600 °C.

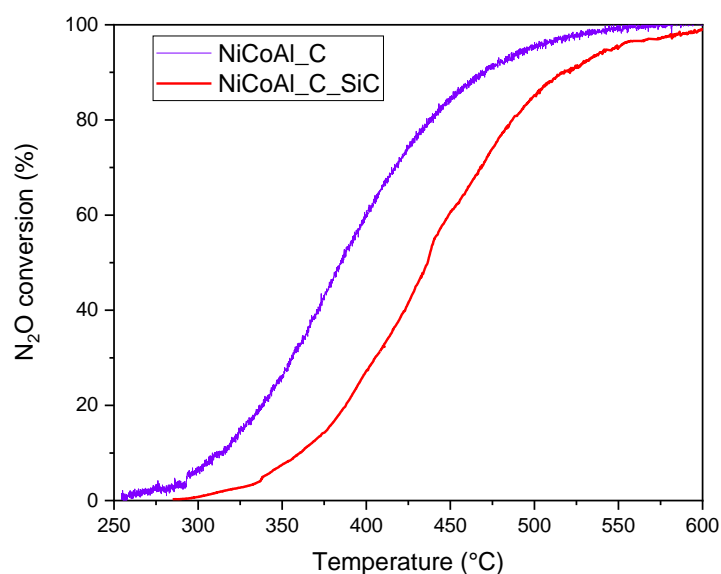


Figure 14. Activity comparison between powder catalyst and structured catalyst. Operating conditions: WHSV = 19 h⁻¹, 1 atm, reagent mixture: 10 vol% N₂O in Ar.

In order to identify the optimal operating conditions to reach a total N₂O conversion, the structured sample was tested at lower WHSV and by using a feeding mixture containing a higher concentration of N₂O. The results (Figure 15) highlighted that the increase in N₂O concentration from 10 vol% to 20 vol%, keeping the space velocity unchanged, does not lead to significant variation of the conversion. Instead, decreasing the WHSV until 5 h⁻¹, the following promising result was achieved: total conversion and selectivity were reached at 510 °C.

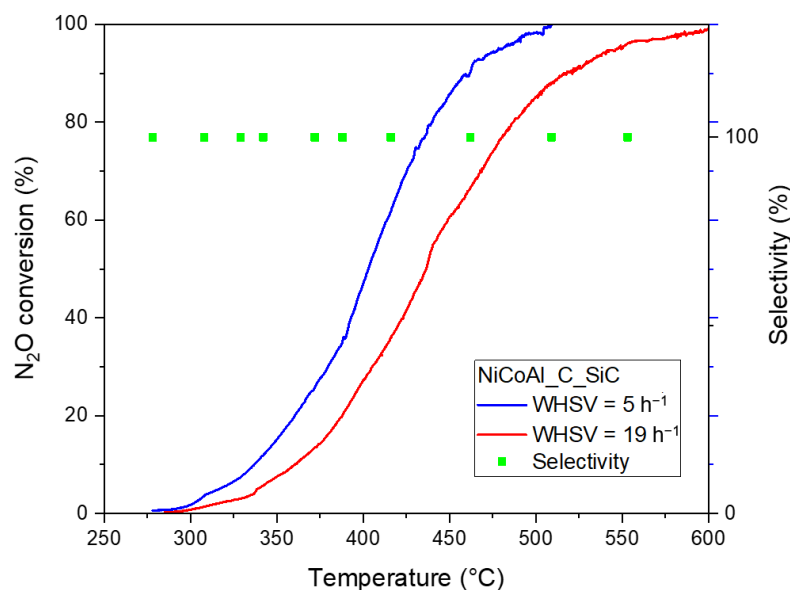


Figure 15. WHSV effect in catalytic N₂O decomposition over NiCoAl_C_SiC structured catalyst (reagent mixture: 20 vol% N₂O in Ar, 1 atm).

3. Materials and Methods

3.1. Catalysts Preparation

In the first phase of the work, two nickel-cobalt powder catalysts were prepared by using the co-precipitation procedure, using two different precipitating agents. To obtain the samples, the following steps were performed: (i) the selected precursor salts were added to known amount of water; (ii) the solution was stirred at room temperature for about 5 min; (iii) a basifying substance was added until the pH of solution reached 9. For all the prepared samples the number of precursor salts was calculated to obtain a Ni/Co ratio equal to 0.3, literature reference value [3], and nickel nitrate and cobalt nitrate were employed as Ni and Co precursors. To achieve precipitation, a 32 vol% NH₃ aqueous solution was employed for NiCo_1 sample and Na₂CO₃, aq 15 wt% for NiCo_2, and the solution was left under stirring for 3 h, then the resultant precipitate was filtered through a filter paper, by using a vacuum pump, and washed until the filtrate was neutral. The differences in preparation are given in Table 2.

Table 2. Resume of the powder samples preparation techniques.

| Sample | Preparation Method | Precursor Salts | Basic Solution |
|-----------|---|--|--|
| NiCo_1 | Co-precipitation, filtration, and wash | Ni(NO ₃) ₂ ·6H ₂ O Co(NO ₃) ₂ ·6H ₂ O | NH _{3,aq} (32 vol%) |
| NiCo_2 | Co-precipitation, filtration, and wash | Ni(NO ₃) ₂ ·6H ₂ O Co(NO ₃) ₂ ·6H ₂ O | Na ₂ CO _{3, aq} (15 wt%) |
| NiCoAl_C | Co-precipitation, filtration, and wash | Ni(NO ₃) ₂ ·6H ₂ O Co(NO ₃) ₂ ·6H ₂ O Al(NO ₃) ₃ ·6H ₂ O | NH _{3, aq} (32 vol%) |
| NiCo_W10% | Direct addition of NiCo_1 to an alumina-based washcoat Al ₂ O ₃ = 10 wt% | | NH _{3, aq} (32 vol%) |
| NiCo_W15% | Direct addition of NiCo_1 to an alumina-based washcoat Al ₂ O ₃ = 15 wt% | | NH _{3, aq} (32 vol%) |
| NiCo_W30% | Direct addition of NiCo_1 to an alumina-based washcoat Al ₂ O ₃ = 30 wt% | | NH _{3, aq} (32 vol%) |

Aiming at the development of the structured catalyst, three washcoat slurries were prepared by mixing the most performing formulation (NiCo_1) with an alumina-based colloidal solution, in three different NiCo/alumina ratios (listed in Table 2), in order to investigate the alumina effect on the catalytic activity. The preparation procedure was as follows.

Water and methylcellulose (1 wt%) were mixed up on a magnetic stirrer at room temperature. When the solution was homogeneous, the pseudoboehmite was added, in an amount such as to obtain the desired ratio with NiCo, and an aqueous solution of ammonia (32 vol%) was added dropwise until the pH of solution reached 9, to obtain a colloidal dispersion. Finally, the catalyst (NiCo_1) was added to the solution, kept under stirring for 24 h. The obtained slurries were heated under stirring until drying, the resulting materials ground and calcined to obtain three powder catalysts.

A fourth alumina-based sample catalyst (NiCoAl_C) was obtained by co-precipitating from an aqueous solution of cobalt nitrate hexahydrate, nickel nitrate hexahydrate, and aluminum nitrate hexahydrate with a mass ratio of 3:3:1 (Co:Ni:Al nitrates). The solution was stirred at room temperature for five minutes, then an aqueous solution of ammonia (32 vol%) was added dropwise until the pH of the solution reached 9. A part of the slurry was filtered through a filter paper, under vacuum, and washed until the filtrate was neutral, to obtain a powder sample.

The six samples obtained were dried overnight at 120 °C (10 °C/min heating rate) in an oven and calcined at 600 °C in air for 2 h (10 °C/min heating rate).

All the catalysts were sieved in order to reach a granulometry of 180–355 µm.

The structured catalyst sample (NiCoAl_C_SiC) was prepared by using a SiC 7 cm long honeycomb monolith as carrier with a square section (1.5 cm × 1.5 cm) composed of 49 through channels. Before depositing the active species, the SiC carrier was pre-treated in air at 1000 °C for 48 h to have a SiO₂ layer on the surface that enhances the slurry adhesion [32]. The most promising Al₂O₃-modified catalytic formulation (NiCoAl_C) was deposited on the monolith by means of dip-coating method as follows: the carrier was dipped in the same slurry used for the NiCoAl_C powder sample preparation, for 20 min, drained to remove the excess, and dried in an oven at 120 °C. The structured sample was calcinated at 600 °C for 3 h (10 °C/min heating rate) to reach chemical and physical stabilization. This procedure was repeated until the mass deposited was about 10% of the total sample weight, so that the catalyst amount deposited was equal to that used for the activity test on the powder sample.

3.2. Catalysts Characterization

The prepared catalysts were characterized by means of different chemical-physical and analytical techniques. The optical analysis was performed by means of a Scanning Electron Microscope (SEM) Philips Mod.XL30 (Amsterdam, the Netherlands), coupled to an Energy Dispersive X-ray Spectrometer (EDS) Oxford (Oxford Instruments, Abingdon, UK). Specific surface areas (SSA) were obtained through N₂ adsorption at −196 °C, by means of NOVAtouch sorptometer (Anton Paar, Graz, Austria), applying BET method. The structural features were evaluated with a Raman spectroscopy using an inVia Raman Microscope (Renishaw, Wotton-under-Edge, UK), equipped with a 514 nm Ar ion laser operating at 25 mW.

The X-ray fluorescence was carried out on the catalysts to evaluate the chemical composition of the samples, by means of the Thermo-Scientific QUANT'X (Thermo Fisher Scientific Inc., Waltham, MA, USA), energy dispersive XRF. The X-ray diffraction (XRD) was performed for the identification and qualitative determination of the crystalline phases in the powder samples. The X-ray diffraction measurements were carried out by means of a Bruker D2 diffractometer (Billerica, MA, USA), designed according to the Bragg geometry. Aiming at the evaluation of the coating layer resistance to a strong mechanical stress, ultrasound adherence test was performed on the structured sample by means of an ultrasonic bath [40,41]. In each cycle of bath, the sample was subjected to the ultrasonic stress for 5 min at room temperature, with a power of 60% compared to the maximum.

The Temperature Programmed Desorption (TPD) of N₂O experimental tests have been performed on two catalytic samples, namely, NiCo_1 and NiCoAl_C. The samples were preliminarily heated in 20 vol% N₂O stream, balanced with Ar, up to 500 °C with a heating rate of 10 °C/min, and then cooled up to room temperature with the same stream. After that, the samples were heated in Ar flow up to 500 °C for detecting the desorbed species.

3.3. Experimental Tests

The experiments of catalytic N₂O decomposition were carried out in a fixed bed configuration. A tubular reactor (17 mm ID and 320 mm long) in AISI 310 stainless steel was employed and located in horizontal position in a furnace for temperature control. This is constituted of three independent heating zones, each with a dedicated K-type thermocouple, therefore optimal temperature control is achieved. The selected amount of catalyst was loaded in the middle section of the reactor, held between two quartz wool disks, while the monolith structured catalyst is placed in the reactor wrapped in a quartz wool layer to avoid bypass phenomena. Two K-type thermocouples were positioned in correspondence with the inlet and outlet section of the catalytic bed, in order to ensure the monitoring of the temperature within the system. The feed stream was adjusted via a mass flow controllers setup. The product stream was analyzed by means of a QGA mass

spectrometer (Hiden Analytical, UK); for a correct quantification of the species, mass-to-charge ratios of 28, 30, 32, 40, 44, 46 (respectively corresponding to nitrogen, nitric oxide, oxygen, argon, nitrous oxide, and nitrogen dioxide) were considered for the analysis.

The catalytic activity tests were carried out over a fixed mass of powder catalyst (1.5 g) and in presence of different gaseous reactant mixtures, using argon as inert gas. The activity of the samples was investigated at different gas hourly space velocity (GHSV) values, varying the inlet concentration of N₂O between 5 and 20 vol% and in presence/absence of oxygen, in 1:1 molar ratio with N₂O. The performance of the structured catalyst was investigated in two different weight hourly space velocity (WHSV) values, calculated with respect to the catalyst amount deposited in order to assure the same contact time of the powder configuration for making the results comparable, and by using two inlet concentration of N₂O corresponding to 10 and 20 vol%. The performances of the catalytic systems were evaluated in terms of the N₂O conversion (X_{N_2O}) and selectivity to N₂ (S_{N_2}). The space velocities GHSV and WHSV, used for the tests with powders and structured catalysts, respectively, were defined as Equations (3) and (4), while N₂O conversion and selectivity to N₂ were defined respectively as Equations (5) and (6), where F_i indicates the molar flow rate of the i -species, and Q is the total volumetric flow rate.

$$GHSV = \frac{Q}{V_{cat}} \quad (3)$$

$$WHSV = \frac{\dot{W}}{g_{cat}} \quad (4)$$

$$X_{N_2O} = \frac{F_{N_2O,in} - F_{N_2O,out}}{F_{N_2O,in}} \times 100\% \quad (5)$$

$$S_{N_2} = \frac{F_{N_2,out}}{F_{N_2,out} + F_{NO_2,out} + F_{NO,out}} \times 100\% \quad (6)$$

The molar flow rate of the components in the outlet gas stream was calculated starting from the corresponding concentrations acquired by the mass spectrometer (as previously described) and by calculating, through the mass balance, the correcting factor to be applied, since this reaction proceeds with a change in the number of moles.

The catalysts were pre-treated by sending an argon stream while heating the system up to 600 °C (10 °C/min heating rate) to remove any impurities adsorbed on the surface of the sample. The experimental tests on the catalysts were carried out in the temperature range 250–650 °C by using a heating rate of 5 °C/min.

4. Conclusions

In the present work, two different nickel-cobalt mixed oxides (Ni_xCo_{1-x}Co₂O₄), active for the N₂O decomposition reaction, were prepared by using ammonia and sodium carbonate as precipitating agents. The results retrieved for the two samples (NiCo_1 and NiCo_2) highlight how the type of precipitating agent can lead to different textural properties and chemical structures in the catalyst and, consequently, to different catalytic activity. Since the sample NiCo_1 exhibited the best N₂O conversion over the whole temperature range, it was employed to prepare catalytic alumina-based formulations with the aim of designing a washcoat slurry to use in the preparation of a structured catalyst for the N₂O decomposition. For reference, a co-precipitated NiCoAl-based catalyst was prepared with the aim of incorporating the alumina into the catalyst structure. The performance of the latter was compared to that of the powder samples, obtained by drying and calcining the three washcoat slurries. The NiCoAl_C sample exhibited the best catalytic performance with a total conversion at 600 °C. Therefore, it was tested under different GHSV conditions (15,000 h⁻¹ and 3000 h⁻¹) and at different N₂O concentrations in order to optimize the operating conditions. Employing a GHSV equal to 3000 h⁻¹, a temperature of 420 °C was needed for obtaining a 100% N₂O conversion, with a total selectivity of N₂. Moreover, by

passing from 10 vol% to 20 vol% of N₂O, the increase in N₂O content did not negatively influence the catalytic activity, in terms of both conversion and selectivity. In conclusion, a structured sample was obtained by depositing the NiCoAl_C catalytic formulation on a SiC honeycomb monolith. The N₂O decomposition was performed with successful results over the structured catalyst by passing a feeding mixture containing 20 vol% of N₂O as follows: total conversion and selectivity were reached at 510 °C. The results obtained with this study represent the following important achievement: the decomposition process of N₂O contained in high concentrations (up to 20 vol%) can be carried out with good performance over NiCoAl-based catalysts, at relatively low temperatures. In particular, the use of a carrier with high thermal conductivity, such as SiC, may result in a more homogeneous temperature distribution inside the catalytic bed, with beneficial effects on the catalytic activity. Therefore, the effective catalytic decomposition of gaseous streams concentrated in N₂O may be obtained also by using structured catalysts, with consequently beneficial effects in terms of the compactness of the reactor and thermal management, as well as resulting in a huge energy savings. Furthermore, the employment of a structured catalyst allows the performance of the process by using a more practical solution suitable for industrial applications.

Author Contributions: Conceptualization, E.M., M.M., S.R., O.M., P.P., F.B. and V.P.; methodology, E.M., M.M., S.R., O.M., P.P., F.B. and V.P.; software, E.M., M.M., S.R., O.M., P.P., F.B. and V.P.; validation, E.M., M.M., S.R., O.M., P.P., F.B. and V.P.; formal analysis, E.M., M.M., S.R., O.M., P.P., F.B. and V.P.; investigation, E.M., M.M., S.R., O.M., P.P., F.B. and V.P.; resources, E.M., M.M., S.R., O.M., P.P., F.B. and V.P.; data curation, E.M., M.M., S.R., O.M., P.P., F.B. and V.P.; writing—original draft preparation, E.M., M.M., S.R., O.M., P.P., F.B. and V.P.; writing—review and editing, E.M., M.M., S.R., O.M., P.P., F.B. and V.P.; visualization, E.M., M.M., S.R., O.M., P.P., F.B. and V.P.; supervision, E.M., M.M., S.R., O.M., P.P., F.B. and V.P.; project administration, E.M., M.M., S.R., O.M., P.P., F.B. and V.P.; funding acquisition, E.M., M.M., S.R., O.M., P.P., F.B. and V.P. All authors have read and agreed to the published version of the manuscript.

Funding: This research received no external funding.

Data Availability Statement: Not applicable.

Acknowledgments: The authors are grateful to Paolo Tramonti for performing the SEM-EDX analysis.

Conflicts of Interest: The authors declare no conflict of interest.

References

1. Li, Y.; Zhang, X.; Zheng, Z. A Review of Transition Metal Oxygen-Evolving Catalysts Decorated by Cerium-Based Materials: Current Status and Future Prospects. *CCS Chem.* **2021**, *3*, 2657–2679. [[CrossRef](#)]
2. Kapteijn, F.; Rodriguez-Mirasol, J.; Moulijn, J.A. Heterogeneous catalytic decomposition of nitrous oxide. *Appl. Catal. B Environ.* **1996**, *9*, 25–64. [[CrossRef](#)]
3. Yan, L.; Ren, T.; Wang, X.; Ji, D.; Suo, J. Catalytic decomposition of N₂O over M_xCo_{1-x}Co₂O₄ (M = Ni, Mg) spinel oxides. *Appl. Catal. B Environ.* **2003**, *45*, 85–90. [[CrossRef](#)]
4. Abu-Zied, B.M. Nitrous oxide decomposition over alkali-promoted magnesium cobaltite catalysts. *Chin. J. Catal.* **2011**, *32*, 264–272. [[CrossRef](#)]
5. van Dijk, E.J.H.; van Loosdrecht, M.C.M.; Pronk, M. Nitrous oxide emission from full-scale municipal aerobic granular sludge. *Water Res.* **2021**, *198*, 117159. [[CrossRef](#)]
6. Li, X.; Chen, J.; Lu, C.; Luo, G.; Yao, H. Mechanism of N₂O generation over chromium poisoned γ -Fe₂O₃ catalyst during selective catalytic reduction of NO_x with NH₃. *Fuel* **2021**, *299*, 120910. [[CrossRef](#)]
7. Alves, L.; Holz, L.I.V.; Fernandes, C.; Ribeirinha, P.; Mendes, D.; Fagg, D.P.; Mendes, A. A comprehensive review of NO_x and N₂O mitigation from industrial streams. *Renew. Sustain. Energy Rev.* **2022**, *155*, 111916. [[CrossRef](#)]
8. Hu, X.; Wang, Y.; Wu, R.; Zhao, L.; Wei, X.; Zhao, Y. Effects of zirconia crystal phases on the catalytic decomposition of N₂O over Co₃O₄/ZrO₂ catalysts. *Appl. Surf. Sci.* **2020**, *514*, 145892. [[CrossRef](#)]
9. Lin, F.; Andana, T.; Wu, Y.; Szanyi, J.; Wang, Y.; Gao, F. Catalytic site requirements for N₂O decomposition on Cu-, Co-, and Fe-SSZ-13 zeolites. *J. Catal.* **2021**, *401*, 70–80. [[CrossRef](#)]
10. Hu, X.; Wang, Y.; Wu, R.; Zhao, Y. N-doped Co₃O₄ catalyst with a high efficiency for the catalytic decomposition of N₂O. *Mol. Catal.* **2021**, *509*, 111656. [[CrossRef](#)]

11. Carabineiro, S.A.C.; Papista, E.; Marnellos, G.E.; Tavares, P.B.; Maldonado-Hódar, F.J.; Konsolakis, M. Catalytic decomposition of N_2O on inorganic oxides: Effect of doping with Au nanoparticles. *Mol. Catal.* **2017**, *436*, 78–89. [[CrossRef](#)]
12. Zhao, T.; Gao, Q.; Liao, W.; Xu, X. Effect of Nd-incorporation and K-modification on catalytic performance of Co_3O_4 for N_2O decomposition. *J. Fuel. Chem. Technol.* **2019**, *47*, 1120–1128. [[CrossRef](#)]
13. Wang, J.; Xia, H.; Ju, X.; Fan, F.; Feng, Z.; Li, C. Catalytic performance of different types of iron zeolites in N_2O decomposition. *Cuihua Xuebao/Chin. J. Catal.* **2013**, *34*, 876–888. [[CrossRef](#)]
14. Alini, S.; Basile, F.; Blasioli, S.; Rinaldi, C.; Vaccari, A. Development of new catalysts for N_2O -decomposition from adipic acid plant. *Appl. Catal. B Environ.* **2007**, *70*, 323–329. [[CrossRef](#)]
15. Xu, M.X.; Wang, H.X.; Ouyang, H.d.; Zhao, L.; Lu, Q. Direct catalytic decomposition of N_2O over bismuth modified NiO catalysts. *J. Hazard. Mater.* **2021**, *401*, 123334. [[CrossRef](#)]
16. Liu, X.; Sheng, L. Catalytic decomposition of N_2O on iron-embedded C_2N monolayer: A DFT study. *Mater. Today Commun.* **2021**, *28*, 102585. [[CrossRef](#)]
17. Grzybek, G.; Gryboś, J.; Indyka, P.; Janas, J.; Ciura, K.; Leszczyński, B.; Zasada, F.; Kotarba, A.; Sojka, Z. Evaluation of the inhibiting effect of H_2O , O_2 , and NO on the performance of laboratory and pilot $K-Zn_xCo_{3-x}O_4$ catalysts supported on $\alpha-Al_2O_3$ for low-temperature N_2O decomposition. *Appl. Catal. B Environ.* **2021**, *297*, 120435. [[CrossRef](#)]
18. Li, S.-X.; Xia, L.; Li, J.-Y.; Liu, X.-G.; Sun, J.-R.; Wang, H.; Chi, Y.-L.; Li, C.-Q.; Song, Y.-J. Effect of alkaline earth metal doping on the catalytic performance of cobalt-based spinel composite metal oxides in N_2O decomposition. *J. Fuel Chem. Technol.* **2018**, *46*, 1377–1385. [[CrossRef](#)]
19. Wang, Y.; Zhou, X.; Wei, X.; Li, X.; Wu, R.; Hu, X.; Zhao, Y. Co/Hydroxyapatite catalysts for N_2O catalytic decomposition: Design of well-defined active sites with geometrical and spacing effects. *Mol. Catal.* **2021**, *501*, 111370. [[CrossRef](#)]
20. Piskorz, W.; Zasada, F.; Stelmachowski, P.; Kotarba, A.; Sojka, Z. Decomposition of N_2O over the surface of cobalt spinel: A DFT account of reactivity experiments. *Catal. Today* **2008**, *137*, 418–422. [[CrossRef](#)]
21. Stelmachowski, P.; Maniak, G.; Kaczmarczyk, J.; Zasada, F.; Piskorz, W.; Kotarba, A.; Sojka, Z. Mg and Al substituted cobalt spinels as catalysts for low temperature deN_2O -Evidence for octahedral cobalt active sites. *Appl. Catal. B Environ.* **2014**, *146*, 105–111. [[CrossRef](#)]
22. Franken, T.; Palkovits, R. Investigation of potassium doped mixed spinels $Cu_xCo_{3-x}O_4$ as catalysts for an efficient N_2O decomposition in real reaction conditions. *Appl. Catal. B Environ.* **2015**, *176–177*, 298–305. [[CrossRef](#)]
23. Yan, L.; Ren, T.; Wang, X.; Gao, Q.; Ji, D.; Suo, J. Excellent catalytic performance of $Zn_xCo_{1-x}Co_2O_4$ spinel catalysts for the decomposition of nitrous oxide. *Catal. Commun.* **2003**, *4*, 505–509. [[CrossRef](#)]
24. Xue, L.; Zhang, C.; He, H.; Teraoka, Y. Catalytic decomposition of N_2O over CeO_2 promoted Co_3O_4 spinel catalyst. *Appl. Catal. B Environ.* **2007**, *75*, 167–174. [[CrossRef](#)]
25. Wang, Y.; Hu, X.; Zheng, K.; Wei, X.; Zhao, Y. Effect of SnO_2 on the structure and catalytic performance of Co_3O_4 for N_2O decomposition. *Catal. Commun.* **2018**, *111*, 70–74. [[CrossRef](#)]
26. Abu-Zied, B.M.; Soliman, S.A.; Abdellah, S.E. Pure and Ni-substituted Co_3O_4 spinel catalysts for direct N_2O decomposition. *Cuihua Xuebao/Chin. J. Catal.* **2014**, *35*, 1105–1112. [[CrossRef](#)]
27. Shimizu, A.; Tanaka, K.; Fujimori, M. Abatement technologies for N_2O emissions in the adipic acid industry. *Chemosphere-Glob. Chang. Sci.* **2000**, *2*, 425–434. [[CrossRef](#)]
28. Konsolakis, M.; Drosou, C.; Yentekakis, I. Support mediated promotional effects of rare earth oxides (CeO_2 and La_2O_3) on N_2O decomposition and N_2O reduction by CO or C_3H_6 over Pt/Al_2O_3 structured catalysts. *Appl. Catal. B Environ.* **2012**, *123–124*, 405–413. [[CrossRef](#)]
29. Suarez, S.; Saiz, C.; Yates, M.; Martin, J.A.; Avila, P.; Blanco, J. Rh/ $\gamma-Al_2O_3$ -sepiolite monolithic catalysts for decomposition of N_2O traces. *Appl. Catal. B Environ.* **2005**, *55*, 57–64. [[CrossRef](#)]
30. Bernauer, M.; Bernauer, B.; Sadovska, G.; Sobalik, Z. High-temperature decomposition of N_2O from the HNO_3 production: Process feasibility using a structured catalyst. *Chem. Eng. Sci.* **2020**, *220*, 115624. [[CrossRef](#)]
31. Palma, V.; Ricca, A.; Martino, M.; Meloni, E. Innovative structured catalytic systems for methane steam reforming intensification. *Chem. Eng. Process. Process Intensif.* **2017**, *120*, 207–215. [[CrossRef](#)]
32. Zhang, H.; Wang, J.; Xu, X. Catalytic decomposition of N_2O over $Ni_xCo_{1-x}CoAlO_4$ spinel oxides prepared by sol-gel method. *J. Fuel. Chem. Technol.* **2015**, *43*, 81–87. [[CrossRef](#)]
33. Bejar, J.; Alvarez-Contreras, L.; Espinosa-Magana, F.; Ledesma-Garcia, J.; Arjona, N.; Arriaga, L.G. Zn-air battery operated with a 3DOM trimetallic spinel ($Mn_{0.5}Ni_{0.5}Co_2O_4$) as the oxygen electrode. *Electrochim. Acta* **2021**, *391*, 138900. [[CrossRef](#)]
34. Zhang, D.; Yan, H.; Lu, Y.; Qiu, K.; Wang, C.; Zhang, Y.; Liu, X.; Luof, J.; Luo, Y. $NiCo_2O_4$ nanostructure materials: Morphology control and electrochemical energy storage. *Dalton Trans.* **2014**, *43*, 15887. [[CrossRef](#)] [[PubMed](#)]
35. Yi, Y.; Zhang, P.; Qin, Z.; Yu, C.; Li, W.; Qin, Q.; Li, B.; Fan, M.; Lianga, X.; Dong, L. Low temperature CO oxidation catalysed by flower-like Ni-Co-O: How physicochemical properties influence catalytic performance. *RSC Adv.* **2018**, *8*, 7110. [[CrossRef](#)]
36. D'Ippolito, V.; Andreozzi, G.B.; Bersanib, D.; Lottici, P.P. Raman fingerprint of chromate, aluminate and ferrite spinels. *Raman Spectrosc.* **2015**, *46*, 1255–1264. [[CrossRef](#)]
37. Huang, Y.; Zhang, S.L.; Lu, X.F.; Wu, Z.P.; Luan, D.; Lou, X.W. Trimetallic Spinel $NiCo_{2-x}Fe_xO_4$ Nanoboxes for Highly Efficient Electrocatalytic Oxygen Evolution. *Angew. Chem. Int. Ed.* **2021**, *60*, 11841–11846. [[CrossRef](#)]

38. Taniou, P.; Ziaka, Z.; Vasileiadis, S. Catalytic Decomposition of N₂O: Best Achievable Methods and Processes. *Am. Trans. Eng. Appl. Sci.* **2013**, *2*, 149–188.
39. Campa, M.; Doyle, A.; Fierro, G. Simultaneous abatement of NO and N₂O with CH₄ over modified Al₂O₃ supported Pt,Pd,Rh. *Catal. Today* **2022**, *384*, 76–87. [[CrossRef](#)]
40. Palma, V.; Pisano, D.; Martino, M.; Ricca, A.; Ciambelli, P. High thermal conductivity structured carriers for catalytic processes intensification. *Chem. Eng. Trans.* **2015**, *43*, 2047–2052. [[CrossRef](#)]
41. Yasaki, S.; Yoshino, Y.; Ihara, K.; Ohkubo, K. Method of Manufacturing an Exhaust Gas Purifying Catalyst. U.S. Patent US 5208206, 4 May 1993.